

# Advantage of probabilistic non-Gaussian operations in the distillation of single mode squeezed vacuum state

Chandan Kumar\*

*Optics and Quantum Information Group, The Institute of Mathematical Sciences,*

*CIT Campus, Taramani, Chennai 600113, India. and*

*Homi Bhabha National Institute, Training School Complex, Anushakti Nagar, Mumbai 400085, India.*

We consider the distillation of squeezing in single mode squeezed vacuum state using three different probabilistic non-Gaussian operations: photon subtraction (PS), photon addition (PA) and photon catalysis (PC). To accomplish this, we consider a practical model to implement these non-Gaussian operations and derive the Wigner characteristic function of the resulting non-Gaussian states. Our result shows that while PS and PC operations can distill squeezing, PA operations cannot. Furthermore, we delve into the success probabilities associated with these non-Gaussian operations and identify optimal parameters for the distillation of squeezing. Our current analysis holds significant relevance for experimental endeavors concerned with squeezing distillation.

## I. INTRODUCTION

Squeezing is an important quantum resource indispensable in various continuous variable quantum information processing (QIP) protocols [1–4], encompassing applications like quantum teleportation [5, 6], quantum metrology [7, 8], and quantum key distribution [9–11]. While a maximum squeezing value of 15 dB has been demonstrated in the infrared wavelength regime [12–14], generating comparably intense squeezed states remains a formidable task in alternative wavelength ranges or different systems [15]. For instance, squeezed states of magnitudes 1.1 dB [16] and 1.3 dB [17] were produced in optomechanical systems, portraying the challenges in producing higher levels of squeezing outside the infrared spectrum. Therefore, it is of paramount importance to find ways to enhance squeezing of the produced state.

Gaussian operations and homodyne detection are ineffective in distilling squeezing of a single mode Gaussian state [18]. This is similar to the case of no-go theorem for entanglement distillation from two-mode Gaussian state via local Gaussian operations [19–21]. Instead, we can resort to probabilistic non-Gaussian operations such as photon subtraction (PS) and photon addition (PA) [22–25] for distillation of squeezing. Essentially, our aim is to prepare an ensemble of small size with high squeezing by selecting few from an ensemble of large size heralded on the successful implementation of non-Gaussian operations. We note that non-Gaussian operations have been utilized to enhance the efficiency of different QIP protocols, including quantum metrology [26–34] and quantum teleportation [35–42]. They have also been used to design quantum heat engine [43–48].

In Ref. [15], multistep distillation scheme was employed to distill squeezing from an ensemble of single mode squeezed vacuum states (SVS). The initial step involved executing two photon subtraction (2-PS) operations on the SVS state. The inquiry arises: Why was

the 2-PS operation specifically chosen? Could a single photon subtraction (1-PS) operation or alternative non-Gaussian operations like PA or photon catalysis (PC) have been utilized for squeezing distillation instead?

To address these questions, we consider a practical model for implementing PS, PA and PC operations on SVS. The generated non-Gaussian states namely photon subtracted SVS (PSSVS), photon added SVS (PASVS), and photon catalyzed SVS (PCSVS) will be collectively referred as NGSVSs. We derive the Wigner characteristic function of the NGSVSs, which is used to evaluate the quadrature squeezing. The investigation into quadrature squeezing reveals distinct outcomes for different non-Gaussian operations as shown in Table I.

TABLE I. Advantage (✓) and disadvantage (✗) of  $n$ -PS,  $n$ -PA, and  $n$ -PC operation in distillation of squeezing

Operation	$n = 1$	$n = 2$	$n = 3$	$n = 4$
PS	✗	✓	✗	✓
PA	✗	✗	✗	✗
PC	✗	✓	✓	✓

We note in particular that the application of two photon catalysis (2-PC) substantially amplifies the squeezing when the initial SVS state exhibits small squeezing.

In most of the theoretical analyses, PS and PA operations are implemented via the annihilation  $\hat{a}$  and creation  $\hat{a}^\dagger$  operator, respectively. However, we departed from this approach by considering a practical model to implement non-Gaussian operations, encompassing PS and PA operations. This model enables us to factor in the success probability associated with non-Gaussian operations, which directly correlates with resource utilization. There are instances where quadrature squeezing can be maximized, yet the success probability is very close to zero. Such circumstances are impractical for experimental implementation. Instead, we propose a trade-off strategy, balancing the enhancement in quadrature squeezing against the success probability to attain optimal scenar-

\* chandan.quantum@gmail.com

ios. We delineate the parameters corresponding to these optimal scenarios.

The subsequent sections of this article are organized as follows. In Sec. II, we have derived the Wigner characteristic function of the SVS state. In Sec. III, we analyze the quadrature squeezing of the NGSVs and also factor the success probability of the non-Gaussian operations. Finally, Sec. IV concludes the main results and provide future directions.

## II. SETUP FOR THE IMPLEMENTATION OF NON-GAUSSIAN OPERATIONS

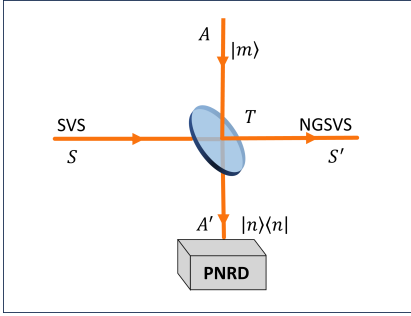


FIG. 1. Setup for the implementation of non-Gaussian operations on the SVS state (explained in detail in the text).

In order to implement different non-Gaussian operations on SVS, we consider the setup shown in Fig. 1. The signal mode (SVS) is mixed with auxiliary mode (Fock state) using a beam splitter of variable transmissivity. Photon number resolving detector is employed on the output mode and a successful detection heralds the implementation of non-Gaussian operation.

We work in phase space and utilize the Wigner characteristic function formalism for convenience in the calculation of moments of the quadrature operators appearing in the quadrature squeezing. Let us consider an  $n$ -mode quantum system with density operator  $\hat{\rho}$ , where the  $i$ th mode has associated quadrature operators  $\hat{q}_i$  and  $\hat{p}_i$ . The Wigner characteristic function of a state with density operator  $\hat{\rho}$  is defined as [3, 49],

$$\chi(\Lambda) = \text{Tr}[\hat{\rho} \exp(-i\Lambda^T \Omega \hat{\xi})], \quad (1)$$

where  $\hat{\xi} = (\hat{q}_1, \hat{p}_1, \dots, \hat{q}_n, \hat{p}_n)^T$ ,  $\Lambda = (\Lambda_1, \Lambda_2, \dots, \Lambda_n)^T$  with  $\Lambda_i = (\tau_i, \sigma_i)^T \in \mathbb{R}^2$ . The symbol  $\Omega$  denotes the symplectic form that is defined as,

$$\Omega = \bigoplus_{k=1}^n \omega = \begin{pmatrix} \omega & & \\ & \ddots & \\ & & \omega \end{pmatrix}, \quad \omega = \begin{pmatrix} 0 & 1 \\ -1 & 0 \end{pmatrix}. \quad (2)$$

For Gaussian states, we require only the first and second order moments. First order moments or the mean

displacement vector  $\bar{\xi}$  can be written as

$$\bar{\xi} = \langle \hat{\xi} \rangle = \text{Tr}[\hat{\rho} \hat{\xi}]. \quad (3)$$

The second order moments can be expressed in the form of a matrix known as covariance matrix  $V$ , which is defined as

$$V = (V_{ij}) = \frac{1}{2} \langle \{\Delta \hat{\xi}_i, \Delta \hat{\xi}_j\} \rangle, \quad (4)$$

where  $\Delta \hat{\xi}_i = \hat{\xi}_i - \langle \hat{\xi}_i \rangle$ , and  $\{\cdot, \cdot\}$  represents anti-commutator. The corresponding Wigner characteristic function is easily obtainable from the following expression [3]:

$$\chi(\Lambda) = \exp[-\frac{1}{2} \Lambda^T (\Omega V \Omega^T) \Lambda - i(\Omega \bar{\xi})^T \Lambda]. \quad (5)$$

We represent the associated quadrature operators of the system mode with  $(\hat{q}_1, \hat{p}_1)$  and that of the auxiliary mode with  $(\hat{q}_2, \hat{p}_2)$ . For the vacuum state, which has the covariance matrix  $V = \text{diag}(1/2, 1/2)$ , the Wigner characteristic function (5) reads

$$\chi_{|0\rangle}(\Lambda_1) = \exp[-(\tau_1^2 + \sigma_1^2)/4]. \quad (6)$$

Under the squeezing transformation characterized by the transformation matrix  $S = \text{diag}(e^{-r}, e^r)$ , the Wigner characteristic function transforms as  $\chi(\Lambda) \rightarrow \chi(S^{-1}\Lambda)$  [3]. Thus, the Wigner characteristic function of the SVS turns out to be

$$\chi_{\text{svs}}(\Lambda_1) = \exp[-(e^{2r}\tau_1^2 + e^{-2r}\sigma_1^2)/4]. \quad (7)$$

Prior to the beam splitter operation, the Wigner characteristic function of the two-mode system is given by

$$\chi_{\text{svs},|m\rangle}(\Lambda) = \chi_{\text{svs}}(\Lambda_1) \chi_{|m\rangle}(\Lambda_2). \quad (8)$$

Here  $\chi_{|m\rangle}(\Lambda_2)$  is the Wigner characteristic function of the Fock state  $|m\rangle$ , which can be evaluated using Eq. (1):

$$\chi_{|m\rangle}(\Lambda_2) = \exp\left[-\frac{\tau_2^2}{4} - \frac{\sigma_2^2}{4}\right] L_m\left(\frac{\tau_2^2}{2} + \frac{\sigma_2^2}{2}\right), \quad (9)$$

where  $L_m(\bullet)$  is the Laguerre polynomial. The transformation matrix corresponding to the beam splitter operation is given by

$$B(T) = \begin{pmatrix} \sqrt{T} \mathbb{1}_2 & \sqrt{1-T} \mathbb{1}_2 \\ -\sqrt{1-T} \mathbb{1}_2 & \sqrt{T} \mathbb{1}_2 \end{pmatrix}, \quad (10)$$

where  $\mathbb{1}_2$  represents the  $2 \times 2$  identity matrix. Post the beam splitter operation, the Wigner characteristic function of the output entangled state can be evaluated as

$$\chi_{\text{out}}(\Lambda) = \chi_{\text{svs},|m\rangle}(B(T)^{-1}\Lambda). \quad (11)$$

A photon number resolving detector measuring  $n$  photons in the output auxiliary mode leads to the generation

of NGSVSSs. The corresponding Wigner characteristic function is given by

$$\chi_{\text{NGSVSSs}}(\Lambda_1) = \frac{1}{2\pi} \int d\Lambda_1 d\Lambda_2 \chi_{\text{out}}(\Lambda) \chi_{|n\rangle}(\Lambda_2). \quad (12)$$

We can write the Fock state using the following identity as

$$\chi_{|k\rangle}(\tau_i, \sigma_i) = \exp \left[ -\frac{\tau_i^2}{4} - \frac{\sigma_i^2}{4} \right] \hat{\mathbf{F}} e^{2uv + u(\tau_i + i\sigma_i) - v(\tau_i - i\sigma_i)}, \quad (13)$$

with

$$\hat{\mathbf{F}} = \frac{1}{2^k k!} \frac{\partial^k}{\partial u^k} \frac{\partial^k}{\partial v^k} \{\bullet\}_{u=v=0}. \quad (14)$$

This enables us to convert the integrand of Eq. (12) into a Gaussian function, which can be easily evaluated. The integral turns out to be

$$\chi_{\text{NGSVSSs}}(\Lambda_1) = a_0 \hat{\mathbf{D}} \exp (\mathbf{\Lambda}^T G_1 \mathbf{\Lambda} + \mathbf{u}^T G_2 \mathbf{\Lambda} + \mathbf{u}^T G_3 \mathbf{u}), \quad (15)$$

where  $a_0 = \sqrt{(1-\lambda^2)/(1-\lambda^2 T^2)}$  with  $\lambda = \tanh r$ . The column vectors are given by  $\mathbf{\Lambda} = (\tau_1, \sigma_1)^T$  and  $\mathbf{u} = (u_1, v_1, u_2, v_2)^T$ . The matrices are:

$$G_1 = \frac{a_0}{-4(1-\lambda^2 T^2)} \begin{pmatrix} (1+\lambda T)^2 & 0 \\ 0 & (1-\lambda T)^2 \end{pmatrix}, \quad (16)$$

$$G_2 = \frac{a_0 \sqrt{1-T}}{1-\lambda^2 T^2} \begin{pmatrix} \lambda T + 1 & -i(\lambda T - 1) \\ -\lambda T - 1 & -i(\lambda T - 1) \\ -\lambda \sqrt{T}(\lambda T + 1) & -i\lambda \sqrt{T}(\lambda T - 1) \\ \lambda \sqrt{T}(\lambda T + 1) & -i\lambda \sqrt{T}(\lambda T - 1) \end{pmatrix}, \quad (17)$$

and

$$G_3 = \frac{a_0}{1-\lambda^2 T^2} \begin{pmatrix} \lambda T(T-1) & 1-T & \lambda \sqrt{T}(1-T) & \sqrt{T}(1-\lambda^2 T) \\ 1-T & \lambda T(T-1) & \sqrt{T}(1-\lambda^2 T) & \lambda \sqrt{T}(1-T) \\ \lambda \sqrt{T}(1-T) & \sqrt{T}(1-\lambda^2 T) & \lambda(T-1) & \lambda^2 T(1-T) \\ \sqrt{T}(1-\lambda^2 T) & \lambda \sqrt{T}(1-T) & \lambda^2 T(1-T) & \lambda(T-1) \end{pmatrix}. \quad (18)$$

The operator  $\hat{\mathbf{D}}$  is defined as

$$\hat{\mathbf{D}} = \frac{2^{-(m+n)}}{m!n!} \frac{\partial^m}{\partial u_1^m} \frac{\partial^m}{\partial v_1^m} \frac{\partial^n}{\partial u_2^n} \frac{\partial^n}{\partial v_2^n} \{\bullet\}_{\substack{u_1=v_1=0 \\ u_2=v_2=0}}. \quad (19)$$

We note that the above Wigner characteristic function is unnormalized (15). The normalized Wigner characteristic function is given by

$$\tilde{\chi}_{\text{NGSVSSs}} = P^{-1} \chi_{\text{NGSVSSs}}. \quad (20)$$

Here  $P$  is the probability given by

$$P = \chi_{\text{NGSVSSs}} \Big|_{\tau_1=\sigma_1=0} = \hat{\mathbf{D}} \exp (\mathbf{u}^T G_3 \mathbf{u}). \quad (21)$$

By choosing specific combinations of  $m$  and  $n$ , we can perform PS, PA and PC operations. When  $m < n$  and  $m > n$ , the SVS undergoes PS and PA operations, respectively, resulting in states labeled as PSSVS and PASVS. In this article, we set  $m = 0$  and  $n = 0$  for PS and PA operations, respectively. As the transmissivity approaches unity, the PS and PA operations become ideal PS ( $\hat{a}_1^n$ ) and ideal PA ( $\hat{a}_1^{\dagger m}$ ) operations. Surprisingly, we observed that the Wigner characteristic function of the 1-PSSVS and 1-PASVS are identical. When  $m = n$  is chosen, the SVS undergoes PC operation, yielding a state labeled as

PCSVS. In the limit of unit transmissivity, the PC operation becomes identity and the PCSVs becomes the SVS.

The Wigner characteristic function of NGSVSSs can be differentiated with respect to  $\tau_1$  and  $\sigma_1$  to obtain the average of symmetrically ordered operators:

$$\langle \hat{q}_1^s \hat{p}_1^t \rangle = \left( \frac{1}{i} \right)^s \left( \frac{1}{-i} \right)^t \frac{\partial^{s+t}}{\partial \sigma_1^s \partial \tau_1^t} \{\tilde{\chi}_{\text{NGSVSSs}}\}_{\tau_1=\sigma_1=0}, \quad (22)$$

where  $\langle \bullet \rangle$  is the notation for symmetric ordering [50].

### III. DISTILLATION OF SQUEEZING

Having evaluated the Wigner characteristic function, we now move to the analysis of quadrature squeezing. The quadrature squeezing in the  $\hat{q}$ -quadrature given by

$$(\Delta q_1)^2 = \langle \hat{q}_1^2 \rangle - \langle \hat{q}_1 \rangle^2. \quad (23)$$

Since  $\hat{q}_1$  and  $\hat{q}_1^2$  are symmetric ordered operators, we can choose appropriate values of  $(s, t)$  in Eq. (22) to calculate the quadrature squeezing. For the SVS,

$$(\Delta q_1)^2_{\text{SVS}} = \exp(-2r) = -\frac{1}{2} + \frac{1}{\lambda + 1}. \quad (24)$$

Our aim is to analyze quadrature squeezing for the NGSVSs, seeking answers to previously posed questions. Specifically, we aim to identify the non-Gaussian operations capable of distilling squeezing.

### A. Quadrature squeezing of 2-PSSVS

We first analyze the case of two photon subtraction ( $m = 0, n = 2$ ), which was utilized in the first step of the multistep distillation scheme [15]. For the 2-PSSVS,

$$(\Delta q_1)_{2\text{-PS}}^2 = -\frac{5}{2} + \frac{5}{\lambda T + 1} + \frac{2(\lambda T - 1)}{2\lambda^2 T^2 + 1}. \quad (25)$$

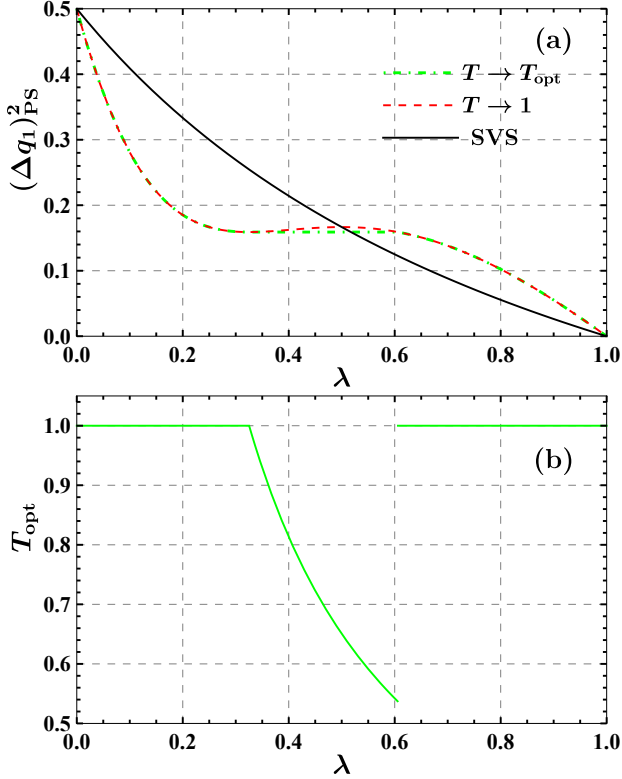


FIG. 2. (a) Quadrature squeezing of 2-PSSVS as a function of squeezing parameter  $\lambda$ . (b) Optimal transmissivity minimizing the quadrature squeezing of 2-PSSVS (25).

In the unit transmissivity limit, the state is ideal 2-PSSVS *i.e.*,  $\mathcal{N}_s \hat{a}^2 |\text{SVS}\rangle$ , which has been analyzed theoretically in Ref. [15]. The corresponding quadrature squeezing can be obtained by taking the unit transmissivity limit in Eq. (25):

$$(\Delta q_1)_{T \rightarrow 1}^2 = -\frac{5}{2} + \frac{5}{\lambda + 1} + \frac{2(\lambda - 1)}{2\lambda^2 + 1}. \quad (26)$$

For unit transmissivity, distillation of squeezing,  $[(\Delta q_1)_{T \rightarrow 1}^2 < (\Delta q_1)_{\text{SVS}}^2]$  is possible when  $\lambda < 1/2$  [15]. For variable transmissivity, the quadrature squeezing (25) is minimized in the unit transmissivity limit

in the range  $\lambda \in \mathcal{S}_1 \equiv (0, 0.33) \cup (0.61, 1)$ . Therefore,  $(\Delta q_1)_{T \rightarrow 1}^2$  is the minimum value in the region  $\mathcal{S}_1$ . In the range  $\lambda \in \mathcal{S}_2 \equiv (0.33, 0.61)$ , squeezing is minimized at

$$T_{\text{opt}} = \frac{-1 - \left(\frac{25}{7+3\sqrt{6}}\right)^{\frac{1}{3}} + (35 + 15\sqrt{6})^{\frac{1}{3}}}{6\lambda}. \quad (27)$$

The corresponding minimized squeezing turns out to be

$$(\Delta q_1)_{T \rightarrow T_{\text{opt}}}^2 = \frac{1 - 5\lambda + 14\lambda^2 - 10\lambda^3}{2(1 + \lambda + 2\lambda^2 + \lambda^3)}. \quad (28)$$

We have pictorially depicted these findings in Fig. 2. It is apparent that the 2-PS operation has the ability to extract squeezing. While quadrature squeezing is not optimized in the unit transmissivity limit in the region  $\mathcal{S}_2$ , the difference between  $(\Delta q_1)_{T \rightarrow T_{\text{opt}}}^2$  and  $(\Delta q_1)_{T \rightarrow 1}^2$  is negligible.

### B. Quadrature squeezing of NGSVSs

In Ref. [15], 2-PS operation was implemented to distill squeezing in the first step of a multistep distillation scheme. Our investigation aims to assess alternative non-Gaussian operations that could potentially substitute the 2-PS operation in such a distillation scheme.

We plot the quadrature squeezing optimized over the transmissivity  $T$  as a function of squeezing  $\lambda$  for different NGSVSs in Fig. 3. The 2-PS and 4-PS operations demonstrate an ability to enhance the quadrature squeezing of the SVS. However, the 1-PS and 3-PS operations result in a reduction of the quadrature squeezing of the SVS. The quadrature squeezing for the 1-PSSVS is

$$(\Delta q_1)_{1\text{-PS}}^2 = -\frac{3}{2} + \frac{3}{1 + \lambda T}. \quad (29)$$

This is minimized in the unit transmissivity limit and  $(\Delta q_1)_{1\text{-PS}}^2 \geq (\Delta q_1)_{\text{SVS}}^2$  holds for  $\lambda \in [0, 1)$ . Therefore, 1-PS cannot distill squeezing. In the zero squeezing and unit transmissivity limit, the quadrature squeezing is

$$\lim_{\substack{\lambda \rightarrow 0 \\ T \rightarrow 1}} (\Delta q_1)_{1\text{-PS}}^2 = \lim_{\substack{\lambda \rightarrow 0 \\ T \rightarrow 1}} (\Delta q_1)_{3\text{-PS}}^2 = \frac{3}{2}. \quad (30)$$

As we noted earlier that 1-PSSVS and 1-PASVS have the same Wigner characteristic function, therefore, 1-PA operation like 1-PS operation cannot distill squeezing. The quadrature squeezing for the 2-PASVS is

$$(\Delta q_1)_{2\text{-PA}}^2 = -\frac{1}{2} + \frac{5}{\lambda T + 1} - \frac{2(2 + \lambda T)}{2 + \lambda^2 T^2}. \quad (31)$$

This is also minimized in the unit transmissivity limit and  $(\Delta q_1)_{2\text{-PA}}^2 \geq (\Delta q_1)_{\text{SVS}}^2$  holds for  $\lambda \in [0, 1)$ . Therefore, 2-PA lacks the ability to distill squeezing. Moreover, the observation from Fig. 3(b) reveals that adding more photons also fails to distill squeezing. In the zero squeezing

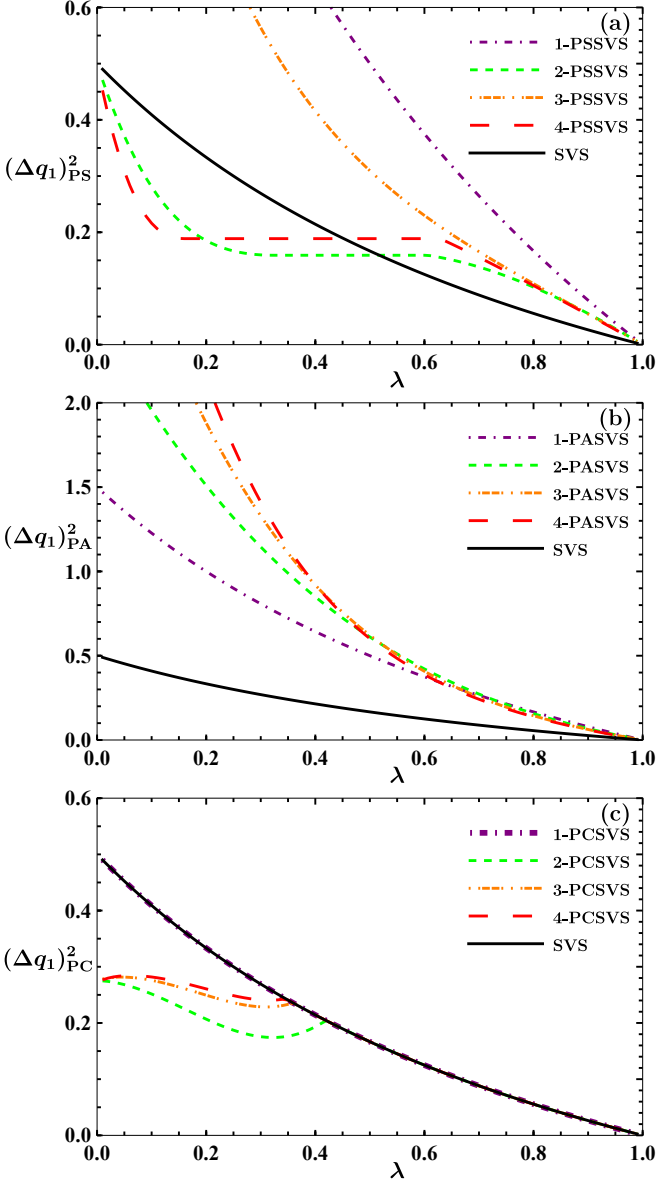


FIG. 3. Quadrature squeezing  $(\Delta q_1)^2$  optimized over the transmissivity as a function of squeezing  $\lambda$  for NGSVSSs.

and unit transmissivity limit, the quadrature squeezing is

$$\lim_{\substack{\lambda \rightarrow 0 \\ T \rightarrow 1}} (\Delta q_1)_{2\text{-PA}}^2 = \frac{5}{2}, \quad \lim_{\substack{\lambda \rightarrow 0 \\ T \rightarrow 1}} (\Delta q_1)_{3\text{-PA}}^2 = \frac{7}{2}. \quad (32)$$

Moving to 1-PC operation, the corresponding quadrature squeezing of the 1-PCSVS state is given by

$$(\Delta q_1)^2 = \left[ \frac{(1 - \lambda T)(1 + 4\lambda + 10\lambda^2 - 4\lambda T - 22\lambda^2 T)}{-4\lambda^3 T + 10\lambda^2 T^2 + 4\lambda^3 T^2 + \lambda^4 T^2} \right] \cdot \frac{2(1 + \lambda T)(1 + 2\lambda^2 - 6\lambda^2 T + 2\lambda^2 T^2 + \lambda^4 T^2)}{.} \quad (33)$$

Quadrature squeezing reaches its minimum in the unit transmissivity limit, where  $(\Delta q_1)_{1\text{-PC}}^2 = (\Delta q_1)_{\text{SVS}}^2$ . Con-

sequently, the 1-PC operation lacks the capacity to distill squeezing. This is in contrast with the fact that 1-PC operation can distill squeezing from mixed state [51, 52].

On the other hand, the 2-PC, 3-PC, and 4-PC operations demonstrate the ability to distill squeezing. These PC operations notably enhance quadrature squeezing by a substantial margin, especially for smaller initial squeezing parameters  $\lambda$ . Among the considered PC operations, the 2-PC operation exhibits the most promising performance.

We have presented the optimal beam splitter transmissivity minimizing the quadrature squeezing as a function of  $\lambda$  in Fig. 4. For PA operation,  $T_{\text{opt}}$  turns out to be unity.

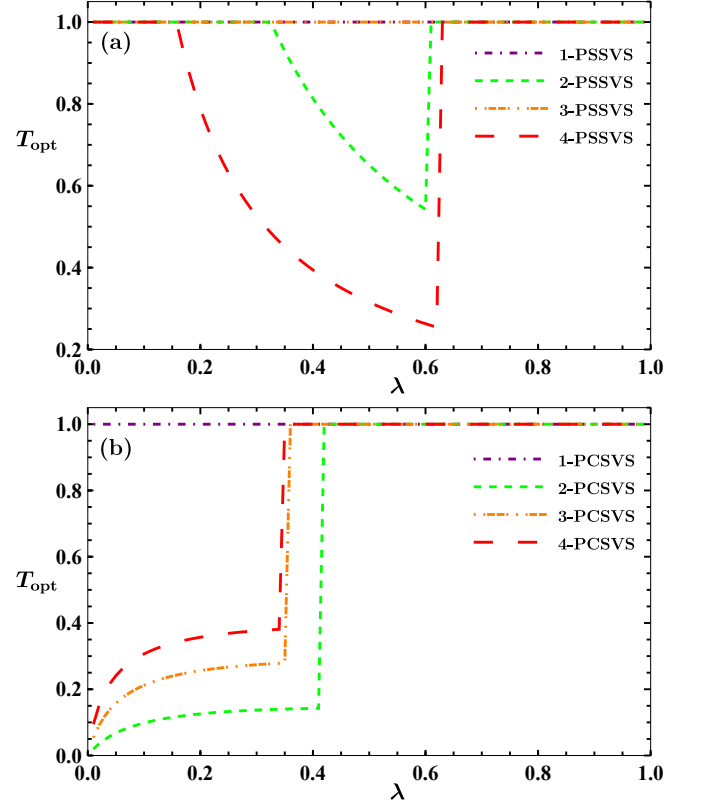


FIG. 4. Optimal beam splitter transmissivity, minimizing the quadrature squeezing  $(\Delta q_1)^2$ , as a function of squeezing  $\lambda$  for NGSVSSs.

It is enlightening to identify the specific range of squeezing and transmissivity parameter rendering distillation of squeezing. To achieve this, we study the enhancement in quadrature squeezing of the generated NGSVSSs in two parameter space namely squeezing and transmissivity. This enhancement, denoted by  $\mathcal{D}_{\text{NG}}$ , is defined as following:

$$\mathcal{D}_{\text{NG}} = (\Delta q_1)_{\text{SVS}}^2 - (\Delta q_1)_{\text{NGSVSS}}^2. \quad (34)$$

Illustrated in Fig. 5 are the plots of  $\mathcal{D}_{\text{NG}}$  for both 2-PSSVS and 2-PCSVS. In the case of 2-PSSVS, squeezing

distillation is viable for low squeezing and high transmissivity values. Conversely, for 2-PCSVS, squeezing can be extracted within the realm of low squeezing and low transmissivity values.

The area within the  $r$  and  $T$  parameter space, where  $\mathcal{D}_{\text{NG}}$  becomes positive, signifies the potential of non-Gaussian operations to distill squeezing.

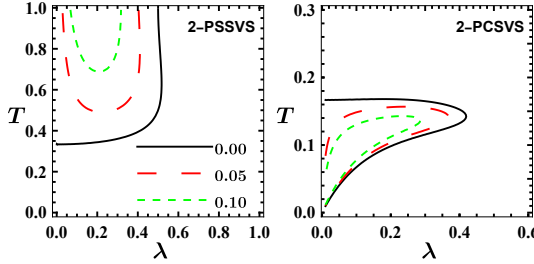


FIG. 5. Curves of fixed  $\mathcal{D}_{\text{NG}}$ , the difference of quadrature squeezing between SVS and NGSVs, as a function of squeezing  $\lambda$  and transmissivity  $T$ .

We have illustrated definite valued curves of the enhancement  $\mathcal{D}_{\text{NG}}$  for both 2-PSSVS and 2-PCSVS in Fig. 5. In the case of 2-PSSVS, the distillation of squeezing is feasible for low squeezing and high transmissivity values. For 2-PCSVS, squeezing can be distilled for low squeezing and low transmissivity values.

### C. Success probability and optimal parameters

As depicted in Fig. 1, the implementation of non-Gaussian operations relies on the detection of a definite photon number by the photon number resolving detector. This introduces a probabilistic nature to the execution of non-Gaussian operations. Consequently, when selecting optimal parameters for a distillation experiment, it is crucial to consider the success probability. To emphasize this aspect, we focus on the 2-PSSVS and illustrate the relationship between the enhancement in quadrature squeezing  $\mathcal{D}_{\text{NG}}$  and the success probability plotted against transmissivity  $T$  in Fig. 6.

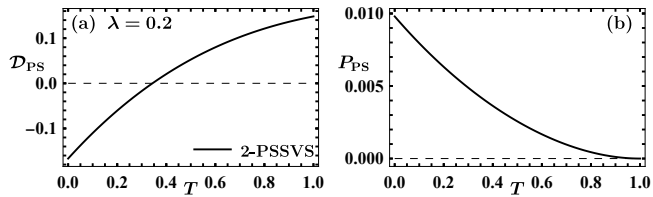


FIG. 6. (a) Enhancement in quadrature squeezing of the original SVS and 2-PSSVS,  $\mathcal{D}_{\text{NG}}$ , as a function of transmissivity  $T$ . (b) Success probability as a function of transmissivity  $T$  for 2-PSSVS.

The analytical expression for the success probability

for the 2-PSSVS is given by

$$P = \frac{\lambda^2(1-T)^2\sqrt{1-\lambda^2}(1+2\lambda^2T^2)}{4(1-\lambda^2T^2)^{5/2}}. \quad (35)$$

The graph illustrates that while the enhancement  $\mathcal{D}_{\text{NG}}$  is maximized in the unit transmissivity limit, the probability tends toward zero under the same conditions. Therefore, aiming to maximize the enhancement  $\mathcal{D}_{\text{NG}}$  results in a scenario unsuitable from an experimental perspective.

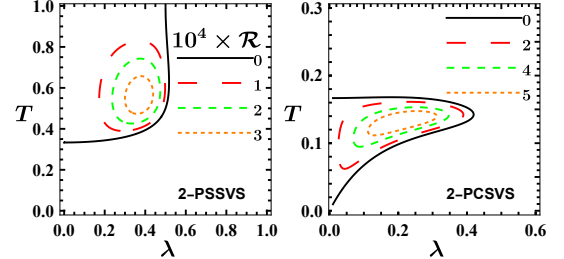


FIG. 7. Curves of fixed magnitude of the product  $\mathcal{R} = \mathcal{D}_{\text{NG}} \times P$  as a function of squeezing  $\lambda$  and transmissivity  $T$ .

To obtain an optimal scenario, we strike a balance between the enhancement in quadrature squeezing  $\mathcal{D}_{\text{NG}}$  and the success probability. To do so, we consider the product  $\mathcal{R}$  defined as  $\mathcal{R} = \mathcal{D}_{\text{NG}} \times P$ . We first plot the product  $\mathcal{R}$  as a function of squeezing and transmissivity in Fig. 7. The curves showcasing the highest magnitude values of  $\mathcal{R}$  enclose a specific region within the  $(r, T)$  space, offering the maximum advantage. Experimental implementation can target the squeezing and transmissivity parameters corresponding to this region. Additionally, in Table II, we present the precise numerical values of the squeezing and transmissivity parameters that maximize the product  $\mathcal{R}$ .

TABLE II. Maximum value of the product  $\mathcal{R}$  and corresponding optimal parameters for different non-Gaussian operations

Operation	$10^4 \times \mathcal{R}_{\text{max}}$	$\lambda_{\text{opt}}$	$T_{\text{opt}}$	$\Delta\phi_{\text{SVS}}$	$\mathcal{D}$	$10^3 \times P$
2-PS	3.6	0.38	0.55	0.23	0.05	7.9
2-PC	5.9	0.22	0.13	0.32	0.12	5.0

For comparison, Ref. [15] considered a squeezing value of  $\lambda = 0.27$  (2.4 dB) and transmissivity  $T = 0.9$ . The corresponding enhancement in quadrature squeezing turns out to be  $\mathcal{D} = 0.12$ , alongside a success probability is  $P = 2.4 \times 10^{-4}$ .

## IV. CONCLUSION

We examined a practical scheme for executing three distinct non-Gaussian operations namely PS, PA and PC

operations on SVS to distill squeezing. Our findings reveal that both PS and PC operations are effective in squeezing enhancement. Particularly noteworthy is the substantial increase in the quadrature squeezing facilitated by 2-PC operation within the low squeezing domain of the SVS state. Our practical scheme enables the consideration of success probability, allowing us to furnish optimal parameters for more efficient resource utilization when factoring in this probability. Our study decisively addresses the potential utilization of other non-

Gaussian operations beyond the 2-PS operation utilized in Ref. [15].

Furthermore, we have furnished the Wigner characteristic function of the NGSVSs, which holds promise for investigating various other nonclassicality measures [57, 58]. These measures encompass evaluations such as of the Mandel- $Q$  parameter [59, 60], manifestations of antibunching effects [61], and assessments of non-Gaussianity [62]. Exploring the impact of these non-Gaussian operations on squeezing distillation in lossy environments shall be taken elsewhere [63–65].

---

[1] S. L. Braunstein and P. van Loock, Quantum information with continuous variables, *Rev. Mod. Phys.* **77**, 513 (2005).

[2] U. Andersen, G. Leuchs, and C. Silberhorn, Continuous-variable quantum information processing, *Laser & Photonics Reviews* **4**, 337 (2010).

[3] C. Weedbrook, S. Pirandola, R. García-Patrón, N. J. Cerf, T. C. Ralph, J. H. Shapiro, and S. Lloyd, Gaussian quantum information, *Rev. Mod. Phys.* **84**, 621 (2012).

[4] G. Adesso, S. Ragy, and A. R. Lee, Continuous variable quantum information: Gaussian states and beyond, *Open Systems & Information Dynamics* **21**, 1440001 (2014).

[5] A. Furusawa, J. L. Sørensen, S. L. Braunstein, C. A. Fuchs, H. J. Kimble, and E. S. Polzik, Unconditional quantum teleportation, *Science* **282**, 706 (1998).

[6] W. P. Bowen, N. Treps, B. C. Buchler, R. Schnabel, T. C. Ralph, H.-A. Bachor, T. Symul, and P. K. Lam, Experimental investigation of continuous-variable quantum teleportation, *Phys. Rev. A* **67**, 032302 (2003).

[7] C. M. Caves, Quantum-mechanical noise in an interferometer, *Phys. Rev. D* **23**, 1693 (1981).

[8] V. Giovannetti, S. Lloyd, and L. Maccone, Quantum-enhanced measurements: Beating the standard quantum limit, *Science* **306**, 1330 (2004).

[9] T. Gehring, V. Händchen, J. Duhme, F. Furrer, T. Franz, C. Pacher, R. F. Werner, and R. Schnabel, Implementation of continuous-variable quantum key distribution with composable and one-sided-device-independent security against coherent attacks, *Nature Communications* **6**, 8795 (2015).

[10] D. Gottesman and J. Preskill, Secure quantum key distribution using squeezed states, *Phys. Rev. A* **63**, 022309 (2001).

[11] S. Pirandola, U. L. Andersen, L. Banchi, M. Berta, D. Bunandar, R. Colbeck, D. Englund, T. Gehring, C. Lupo, C. Ottaviani, J. L. Pereira, M. Razavi, J. S. Shaari, M. Tomamichel, V. C. Usenko, G. Vallone, P. Villoresi, and P. Wallden, Advances in quantum cryptography, *Adv. Opt. Photon.* **12**, 1012 (2020).

[12] H. Vahlbruch, M. Mehmet, S. Chelkowski, B. Hage, A. Franzen, N. Lastzka, S. Goßler, K. Danzmann, and R. Schnabel, Observation of squeezed light with 10-db quantum-noise reduction, *Phys. Rev. Lett.* **100**, 033602 (2008).

[13] M. Mehmet, S. Ast, T. Eberle, S. Steinlechner, H. Vahlbruch, and R. Schnabel, Squeezed light at 1550 nm with a quantum noise reduction of 12.3 db, *Opt. Express* **19**, 25763 (2011).

[14] H. Vahlbruch, M. Mehmet, K. Danzmann, and R. Schnabel, Detection of 15 db squeezed states of light and their application for the absolute calibration of photoelectric quantum efficiency, *Phys. Rev. Lett.* **117**, 110801 (2016).

[15] S. Grebien, J. Götsch, B. Hage, J. Fiurášek, and R. Schnabel, Multistep two-copy distillation of squeezed states via two-photon subtraction, *Phys. Rev. Lett.* **129**, 273604 (2022).

[16] L. Magrini, V. A. Camarena-Chávez, C. Bach, A. Johnson, and M. Aspelmeyer, Squeezed light from a levitated nanoparticle at room temperature, *Phys. Rev. Lett.* **129**, 053601 (2022).

[17] A. Militaru, M. Rossi, F. Tebbenjohanns, O. Romero-Isart, M. Frimmer, and L. Novotny, Ponderomotive squeezing of light by a levitated nanoparticle in free space, *Phys. Rev. Lett.* **129**, 053602 (2022).

[18] B. Kraus, K. Hammerer, G. Giedke, and J. I. Cirac, Entanglement generation and hamiltonian simulation in continuous-variable systems, *Phys. Rev. A* **67**, 042314 (2003).

[19] J. Eisert, S. Scheel, and M. B. Plenio, Distilling gaussian states with gaussian operations is impossible, *Phys. Rev. Lett.* **89**, 137903 (2002).

[20] J. Fiurášek, Gaussian transformations and distillation of entangled gaussian states, *Phys. Rev. Lett.* **89**, 137904 (2002).

[21] G. Giedke and J. Ignacio Cirac, Characterization of gaussian operations and distillation of gaussian states, *Phys. Rev. A* **66**, 032316 (2002).

[22] A. Ourjoumtsev, A. Dantan, R. Tualle-Brouri, and P. Grangier, Increasing entanglement between gaussian states by coherent photon subtraction, *Phys. Rev. Lett.* **98**, 030502 (2007).

[23] H. Takahashi, J. S. Neergaard-Nielsen, M. Takeuchi, M. Takeoka, K. Hayasaka, A. Furusawa, and M. Sasaki, Entanglement distillation from gaussian input states, *Nature Photonics* **4**, 178 (2010).

[24] Y. Kurochkin, A. S. Prasad, and A. I. Lvovsky, Distillation of the two-mode squeezed state, *Phys. Rev. Lett.* **112**, 070402 (2014).

[25] T. Dirmeier, J. Tiedau, I. Khan, V. Ansari, C. R. Müller, C. Silberhorn, C. Marquardt, and G. Leuchs, Distillation of squeezing using an engineered pulsed parametric down-conversion source, *Opt. Express* **28**, 30784 (2020).

[26] R. Birrittella, J. Mimih, and C. C. Gerry, Multiphoton quantum interference at a beam splitter and the approach to heisenberg-limited interferometry, *Phys. Rev. A* **86**,

063828 (2012).

[27] R. Carranza and C. C. Gerry, Photon-subtracted two-mode squeezed vacuum states and applications to quantum optical interferometry, *J. Opt. Soc. Am. B* **29**, 2581 (2012).

[28] D. Braun, P. Jian, O. Pinel, and N. Treps, Precision measurements with photon-subtracted or photon-added gaussian states, *Phys. Rev. A* **90**, 013821 (2014).

[29] Y. Ouyang, S. Wang, and L. Zhang, Quantum optical interferometry via the photon-added two-mode squeezed vacuum states, *J. Opt. Soc. Am. B* **33**, 1373 (2016).

[30] H. Zhang, W. Ye, C. Wei, Y. Xia, S. Chang, Z. Liao, and L. Hu, Improved phase sensitivity in a quantum optical interferometer based on multiphoton catalytic two-mode squeezed vacuum states, *Phys. Rev. A* **103**, 013705 (2021).

[31] S.-H. Tan, B. I. Erkmen, V. Giovannetti, S. Guha, S. Lloyd, L. Maccone, S. Pirandola, and J. H. Shapiro, Quantum illumination with gaussian states, *Phys. Rev. Lett.* **101**, 253601 (2008).

[32] E. D. Lopaeva, I. Ruo Berchera, I. P. Degiovanni, S. Olivares, G. Brida, and M. Genovese, Experimental realization of quantum illumination, *Phys. Rev. Lett.* **110**, 153603 (2013).

[33] C. Kumar, Rishabh, and S. Arora, Enhanced phase estimation in parity-detection-based mach-zehnder interferometer using non-gaussian two-mode squeezed thermal input state, *Annalen der Physik* **535**, 2300117 (2023).

[34] C. Kumar, Rishabh, M. Sharma, and S. Arora, Parity-detection-based mach-zehnder interferometry with coherent and non-gaussian squeezed vacuum states as inputs, *Phys. Rev. A* **108**, 012605 (2023).

[35] T. Opatrný, G. Kurizki, and D.-G. Welsch, Improvement on teleportation of continuous variables by photon subtraction via conditional measurement, *Phys. Rev. A* **61**, 032302 (2000).

[36] F. Dell'Anno, S. De Siena, L. Albano, and F. Illuminati, Continuous-variable quantum teleportation with non-gaussian resources, *Phys. Rev. A* **76**, 022301 (2007).

[37] Y. Yang and F.-L. Li, Entanglement properties of non-gaussian resources generated via photon subtraction and addition and continuous-variable quantum-teleportation improvement, *Phys. Rev. A* **80**, 022315 (2009).

[38] X.-x. Xu, Enhancing quantum entanglement and quantum teleportation for two-mode squeezed vacuum state by local quantum-optical catalysis, *Phys. Rev. A* **92**, 012318 (2015).

[39] L. Hu, Z. Liao, and M. S. Zubairy, Continuous-variable entanglement via multiphoton catalysis, *Phys. Rev. A* **95**, 012310 (2017).

[40] S. Wang, L.-L. Hou, X.-F. Chen, and X.-F. Xu, Continuous-variable quantum teleportation with non-gaussian entangled states generated via multiple-photon subtraction and addition, *Phys. Rev. A* **91**, 063832 (2015).

[41] C. Kumar and S. Arora, Success probability and performance optimization in non-gaussian continuous-variable quantum teleportation, *Phys. Rev. A* **107**, 012418 (2023).

[42] C. Kumar, M. Sharma, and S. Arora, Continuous variable quantum teleportation in a dissipative environment: Comparison of non-gaussian operations before and after noisy channel, *arXiv:2212.13133* (2022).

[43] M. D. Vidrighin, O. Dahlsten, M. Barbieri, M. S. Kim, V. Vedral, and I. A. Walmsley, Photonic maxwell's demon, *Phys. Rev. Lett.* **116**, 050401 (2016).

[44] J. Hloušek, M. Ježek, and R. Filip, Work and information from thermal states after subtraction of energy quanta, *Scientific Reports* **7**, 13046 (2017).

[45] A. Shu, J. Dai, and V. Scarani, Power of an optical maxwell's demon in the presence of photon-number correlations, *Phys. Rev. A* **95**, 022123 (2017).

[46] G. L. Zanin, M. Antesberger, M. J. Jacquet, P. H. S. Ribeiro, L. A. Rozema, and P. Walther, Enhanced Photonic Maxwell's Demon with Correlated Baths, *Quantum* **6**, 810 (2022).

[47] S. Zhang, Optical maxwell's demon phase space theory and its efficiency improvement to 90 squeezing, in *2021 13th International Conference on Wireless Communications and Signal Processing (WCSP)* (2021) pp. 1–5.

[48] G. Tatsi, D. W. Canning, U. Zanforlin, L. Mazzarella, J. Jeffers, and G. S. Buller, Manipulating thermal light via displaced-photon subtraction, *Phys. Rev. A* **105**, 053701 (2022).

[49] S. Olivares, Quantum optics in the phase space, *The European Physical Journal Special Topics* **203**, 3 (2012).

[50] S. M. Barnett and P. M. Radmore, *Methods in Theoretical Quantum Optics* (Oxford University Press, Oxford, 2002).

[51] A. I. Lvovsky and J. Mlynek, Quantum-optical catalysis: Generating nonclassical states of light by means of linear optics, *Phys. Rev. Lett.* **88**, 250401 (2002).

[52] A. E. Ulanov, I. A. Fedorov, A. A. Pushkina, Y. V. Kurochkin, T. C. Ralph, and A. I. Lvovsky, Undoing the effect of loss on quantum entanglement, *Nature Photonics* **9**, 764 (2015).

[53] C. M. Nunn, J. D. Franson, and T. B. Pittman, Modifying quantum optical states by zero-photon subtraction, *Phys. Rev. A* **105**, 033702 (2022).

[54] C. M. Nunn, S. U. Shringarpure, and T. B. Pittman, Transforming photon statistics through zero-photon subtraction, *Phys. Rev. A* **107**, 043711 (2023).

[55] H. Zhong, Y. Guo, Y. Mao, W. Ye, and D. Huang, Virtual zero-photon catalysis for improving continuous-variable quantum key distribution via gaussian post-selection, *Scientific Reports* **10**, 17526 (2020).

[56] C. N. Gagatsos, J. Fiurášek, A. Zavatta, M. Bellini, and N. J. Cerf, Heralded noiseless amplification and attenuation of non-gaussian states of light, *Phys. Rev. A* **89**, 062311 (2014).

[57] K. Thapliyal, N. L. Samantray, J. Banerji, and A. Pathak, Comparison of lower- and higher-order nonclassicality in photon added and subtracted squeezed coherent states, *Physics Letters A* **381**, 3178 (2017).

[58] P. Malpani, N. Alam, K. Thapliyal, A. Pathak, V. Narayanan, and S. Banerjee, Lower- and higher-order nonclassical properties of photon added and subtracted displaced fock states, *Annalen der Physik* **531**, 1800318 (2019).

[59] L. Mandel, Sub-poissonian photon statistics in resonance fluorescence, *Opt. Lett.* **4**, 205 (1979).

[60] A. Biswas and G. S. Agarwal, Nonclassicality and decoherence of photon-subtracted squeezed states, *Phys. Rev. A* **75**, 032104 (2007).

[61] C. T. Lee, Many-photon antibunching in generalized pair coherent states, *Phys. Rev. A* **41**, 1569 (1990).

[62] M. G. Genoni, M. G. A. Paris, and K. Banaszek, Quantifying the non-gaussian character of a quantum state by quantum relative entropy, *Phys. Rev. A* **78**, 060303

(2008).

- [63] L.-y. Hu, X.-x. Xu, Z.-s. Wang, and X.-f. Xu, Photon-subtracted squeezed thermal state: Nonclassicality and decoherence, *Phys. Rev. A* **82**, 043842 (2010).
- [64] A. E. Ulanov, I. A. Fedorov, A. A. Pushkina, Y. V. Kurochkin, T. C. Ralph, and A. I. Lvovsky, Undoing the effect of loss on quantum entanglement, *Nature Photonics* **9**, 764 (2015).
- [65] R. Meena and S. Banerjee, Characterization of quantumness of non-gaussian states under the influence of gaussian channel, *Quantum Information Processing* **22**, 298 (2023).